Supplementary Information

Nanoscale Solid State Batteries Enabled By Thermal Atomic Layer Deposition of a Lithium Polyphosphazene Solid State Electrolyte

Alexander J. Pearse[†], Thomas E. Schmitt[†], Elliot J. Fuller[‡], Farid El-Gabaly[‡], Chuan-Fu Lin[†], Konstantinos Gerasopoulos[⩩], Alexander C. Kozen[⌟], A. Alec Talin[‡], Gary Rubloff[†], Keith E. Gregorcyzck*[†]*

[†]Department of Materials Science and Engineering, University of Maryland, College Park, MD 20740

[⩩] Research and Exploratory Development Department, The Johns Hopkins University Applied Physics Laboratory, Laurel, MD 20723

[⌟] American Society for Engineering Education, residing at the U.S. Naval Research Laboratory 1818 N St NW, Suite 600 Washington DC, 20036

[‡]Sandia National Laboratories, Livermore, CA 94551

Figure S1: Diagram of the Integrated System

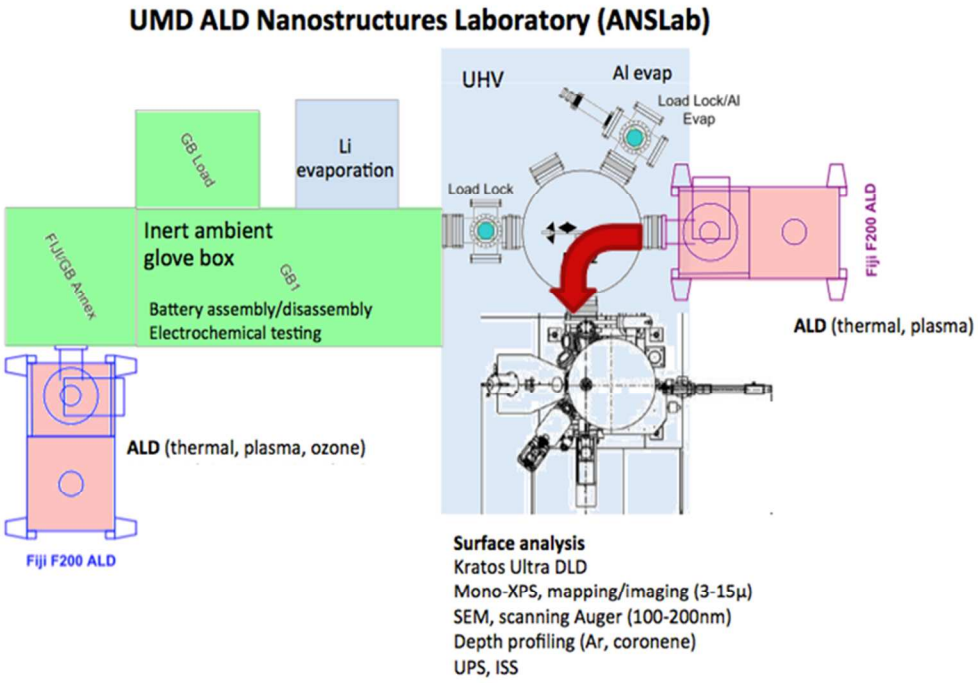

Figure S1: A schematic of the integrated vacuum/deposition system used for experiments described in the main text. ALD-grown samples can be transferred directly from the ALD chamber to the XPS in UHV via the red arrow.

Table S1: Detailed Fitting Parameters for PEIS taken at 35C

Sample ID	LPZ Thickness (nm)	R_b (Ω)	R_r (Ω)	CPE_b Q	CPE_b *n*	CPE_r Q	CPE_r *n*	χ^2
LPZ-300 (Pt/Pt)	80	1085	5386	9.02×10^{-9}	0.899	9.16×10^{-8}	0.795	2.3×10^{-4}
LPZ-250 (Pt/Pt)	70	1448	5049	7.93×10^{-9}	0.903	1.32×10^{-7}	0.783	2.4×10^{-4}
LPZ-300 (Pt/Li)	90	1749	—	8.91×10^{-9}	0.864	—	—	1.3×10^{-4}

Table S1 lists the parameters used to model the ionic conductivity of ALD LPZ films at 35C, which includes a component associated with the film bulk (R_b and CPE_b) and the Li_2CO_3 reaction layer in the case of air exposed films (R_r and CPE_r). The constant phase element impedance is a generalized capacitance and is described by the equation

$$Z = \frac{1}{Q\omega^n} \mathrm{e}^{-i\pi n/2}$$

and the associated values for Q and n are listed in the table. χ2 describes the goodness of fit for each model.

Figure S2: In-Situ SE of DEPA Pulses Alone at 300C

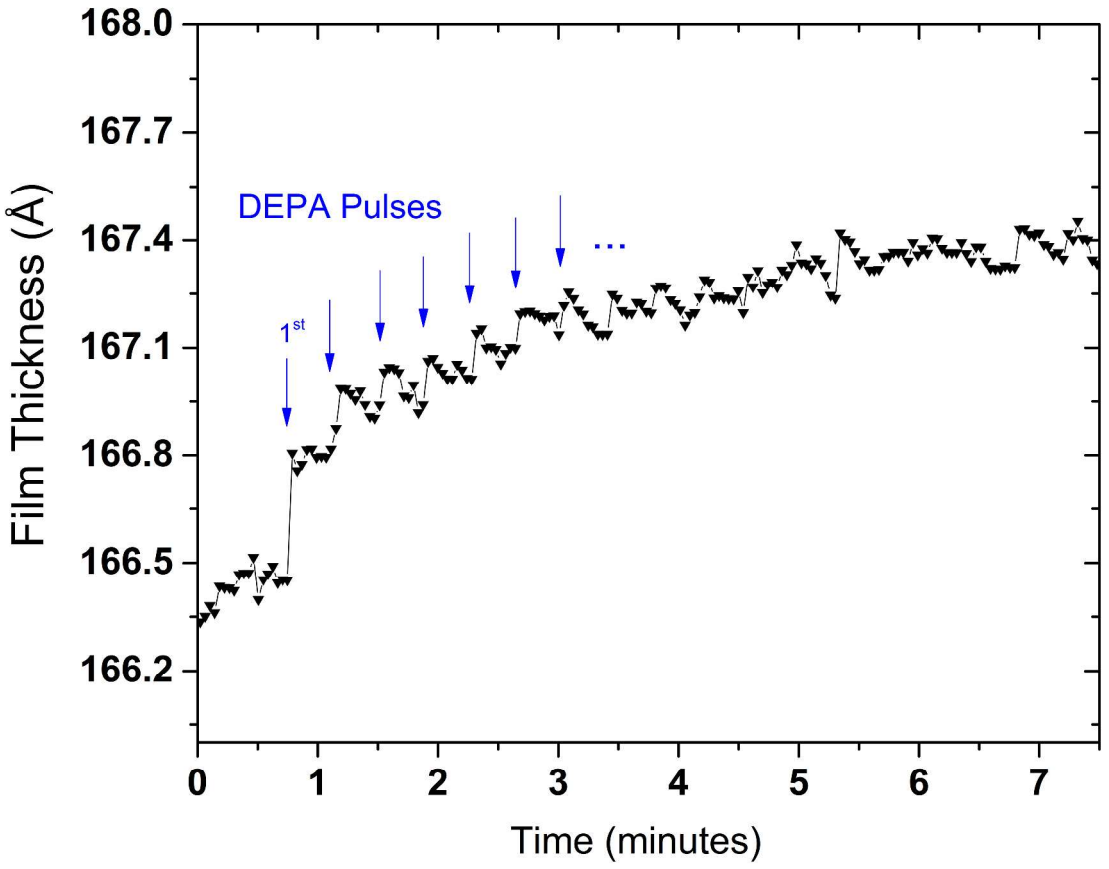

Figure S2: In-situ ellipsometry of film growth while pulsing DEPA only (no LiO^{t}Bu pulses) at 300C on a pre-grown LPZ-300 surface 16.6 nm in thickness. The blue arrows mark the locations in time of 2s DEPA pulses (separated by 30 seconds and which continue during the entire plotted time period). The first pulse results in the strongest change measured by SE, and subsequent pulses contribute smaller and smaller differential changes in film thickness before saturating at a total change of ~ 1 angstrom. This indicates that DEPA alone does not form a film.

Figure S3: Gas Cluster Source XPS Depth Profile of Air-Exposed ALD LPZ

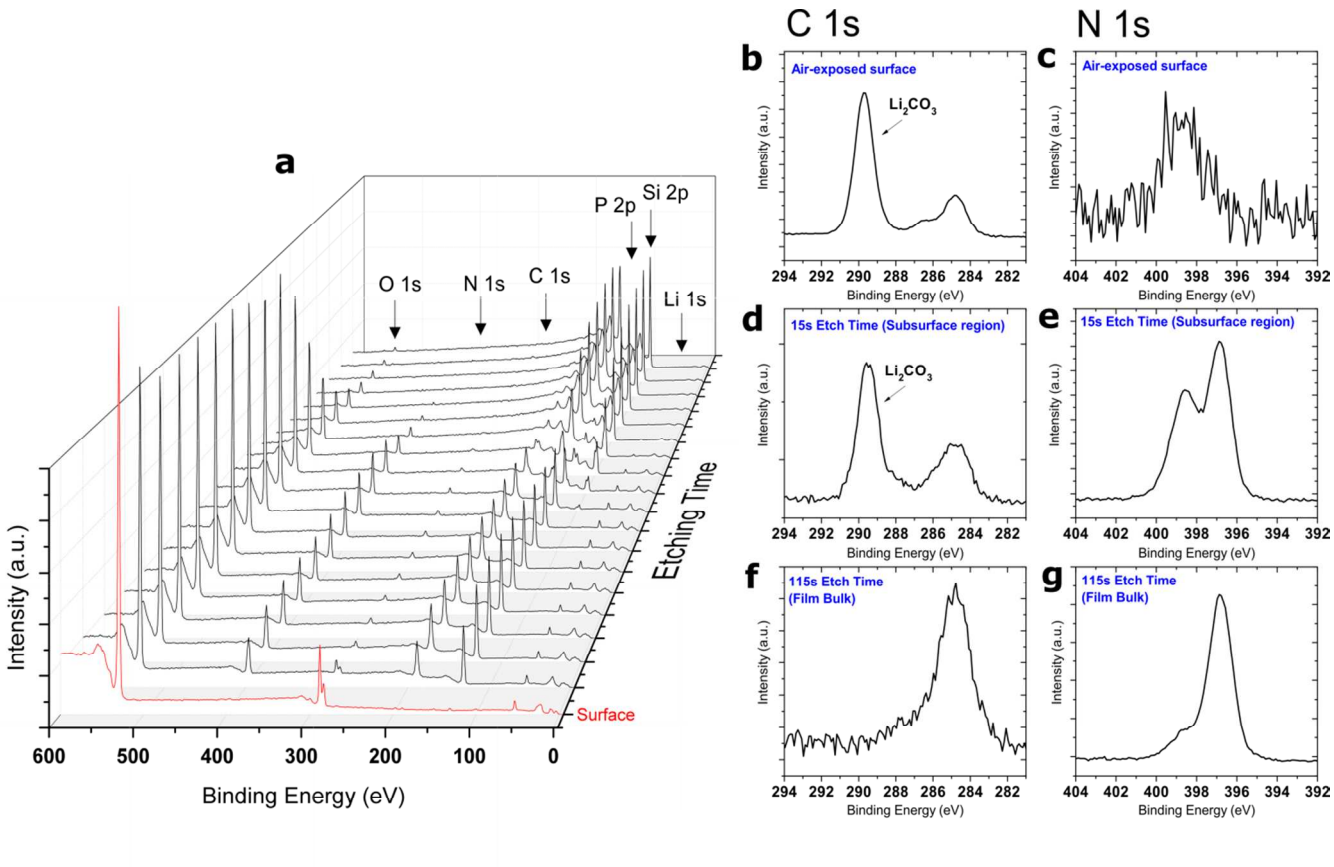

Figure S1: Data from an XPS depth profile of an air-exposed ALD LPZ-300 film grown on a Si substrate (total thickness ~50nm). (a) Survey spectra plotted as a function of etching time (b-g) High resolution spectra of the C 1s and N 1s core levels taken at the surface (b,c) after one etch cycle (d,e) and from the bulk of the film (f,g). High resolution spectra are calibrated to the hydrocarbon component at 284.8 eV.

Figure S2 shows the presence of a decomposed/reacted surface layer formed in air-exposed ALD LPZ films. The C 1s core level spectra taken from the surface (Figure S3b) and just below the surface (Figure S3d) clearly show the presence of a carbon species at 289.7 eV, which is characteristic of lithium carbonate.[1] The N chemistry of the film is also affected near the surface, with increasing N content associated with the N ε component identified in Figure 2 in the main text. After several etching cycles, the chemistry again resembles that measured for pristine films (Figure S3f,g). The thickness of the reaction layer can be estimated to be on the order of a few nm.

We found that normal monoatomic ion sputtering sources significantly degraded the film. As a result, the XPS/GCIS analyses were carried out with a Kratos AXIS Supra spectrometer equipped with a Gas Cluster Ion Source (GCIS) for sample sputtering using Ar_n^+ cluster ions or monatomic Ar^+. Clusters are created in the GCIS via the supersonic expansion of high pressure Ar gas through a de Laval nozzle into a medium vacuum region. Nascent clusters are transmitted through a differentially pumped region into an electron impact ionisation source. Following ionisation, Ar_n^+ cluster ions are extracted through the length of a Wien filter to eliminate all small ions and limit the transmitted cluster size distribution spread around a chosen median value. The Ar_n^+ cluster ions are then deflected through 2° to eliminate neutral and metastable species from the beam before simultaneous focusing and rastering across the sample. Alternately, Ar gas can be directly introduced into the electron impact ionisation source to allow production of monoatomic Ar^+ ions. The GCIS can deliver Ar_n^+ cluster ions at energies from 0.25–20 keV and cluster sizes n = 150–5000.

Figure S4: TEM Damage of ALD LPZ

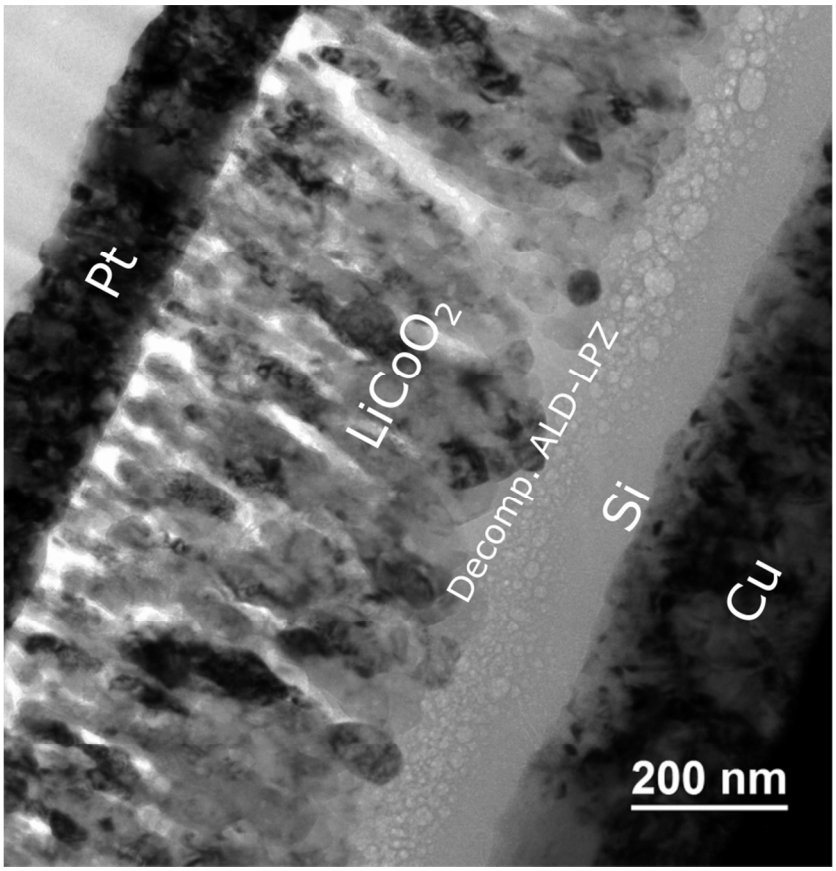

Figure S4: TEM image of a cross-sectioned LCO/LPZ-300/Si battery after extended exposure to the electron beam. The LPZ layer decomposes and forms bubbles, likely through gas evolution. This allows for easy visual differentiation of the LPZ and Si layers.

Figure S5: First cycle capacity loss in LCO/LiPON/Si batteries using RF-sputtered LiPON

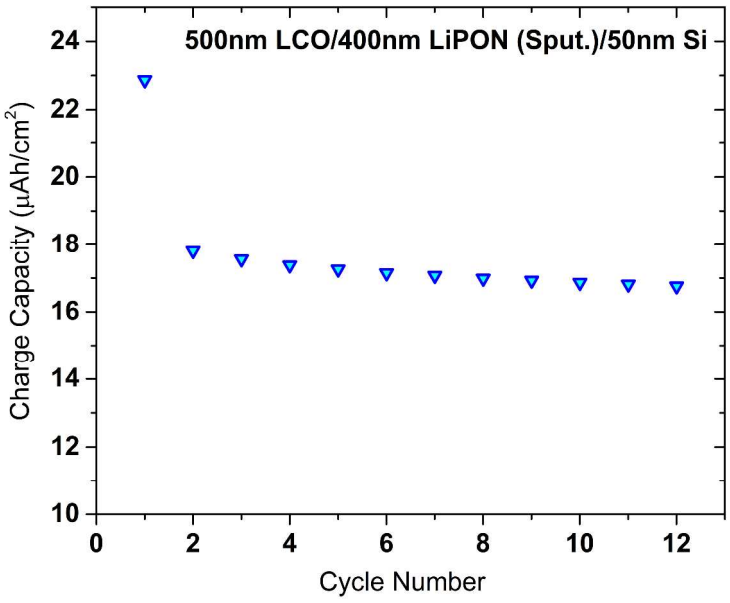

Figure S5: Charge capacity at a C/10 rate of a SSB made with 500nm LCO, 400nm RF-sputtered LiPON (made using previously published procedures), and 50nm Si.[2] The battery was cycled between 3 and 4.2V. These devices show a similar first cycle capacity loss and stable capacity to batteries made using ALD LPZ, which indicates the majority of the irreversible capacity is likely associated with the Si anode and not the electrolyte.

Figure S6: SEM of Surface Reaction Layer in Cycled Batteries

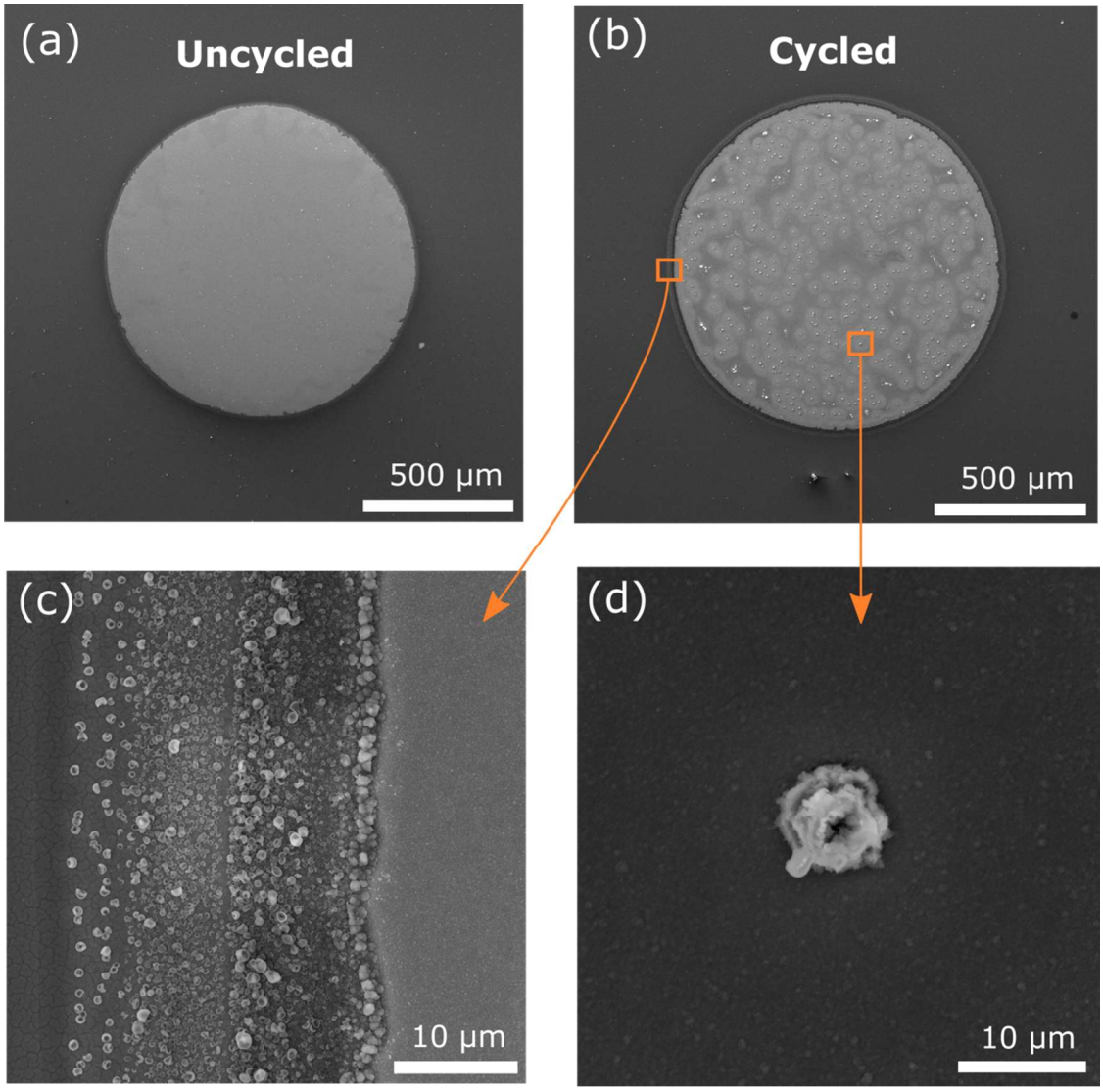

Figure S6: SEM images of (a) an as made, uncycled battery and (b) a cycled battery. The battery chemistry is identical to the devices described in Figures 6 and 7 of the main text. Cycled devices evolve debris both on the surface (d) and near the edges (c) of the Cu current collector, which we believe to be lithium compounds formed from the reaction of mobile lithium inserted into the Si anode and environmental contaminants, including trace H_2O and O_2 in the glovebox. This may be one source of capacity loss over time, and future devices will be encapsulated to help prevent this effect.

Figure S7: XRD of LPZ-300

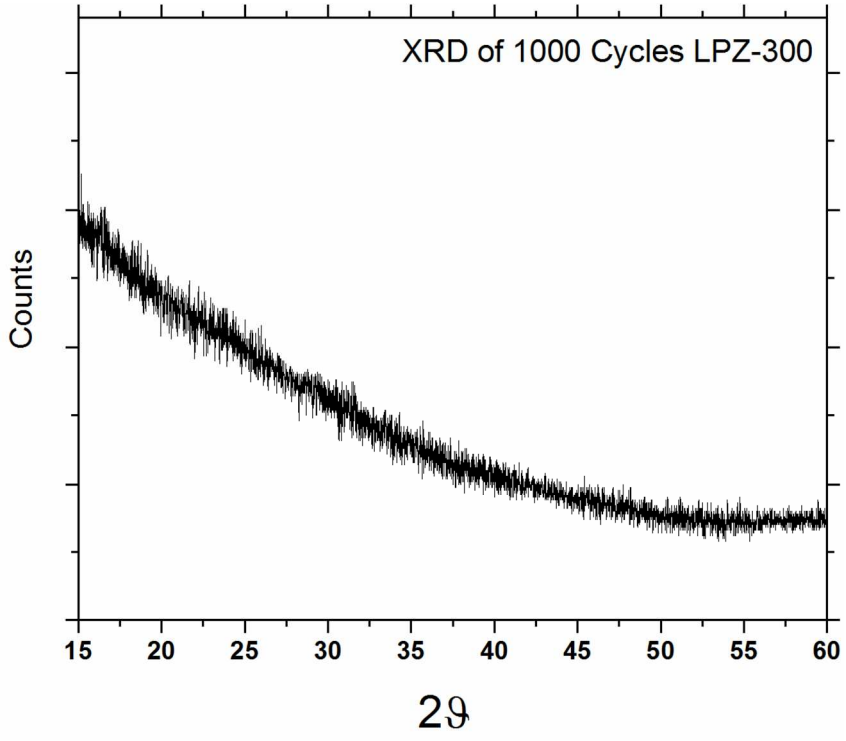

Figure S7: XRD of a LPZ-300 sample showing the amorphous nature of the films. This corresponds well to the lack of structure identifiable in TEM cross section studies.

Figure S8: Transport Characteristics of ALD LPZ After Long Term Storage

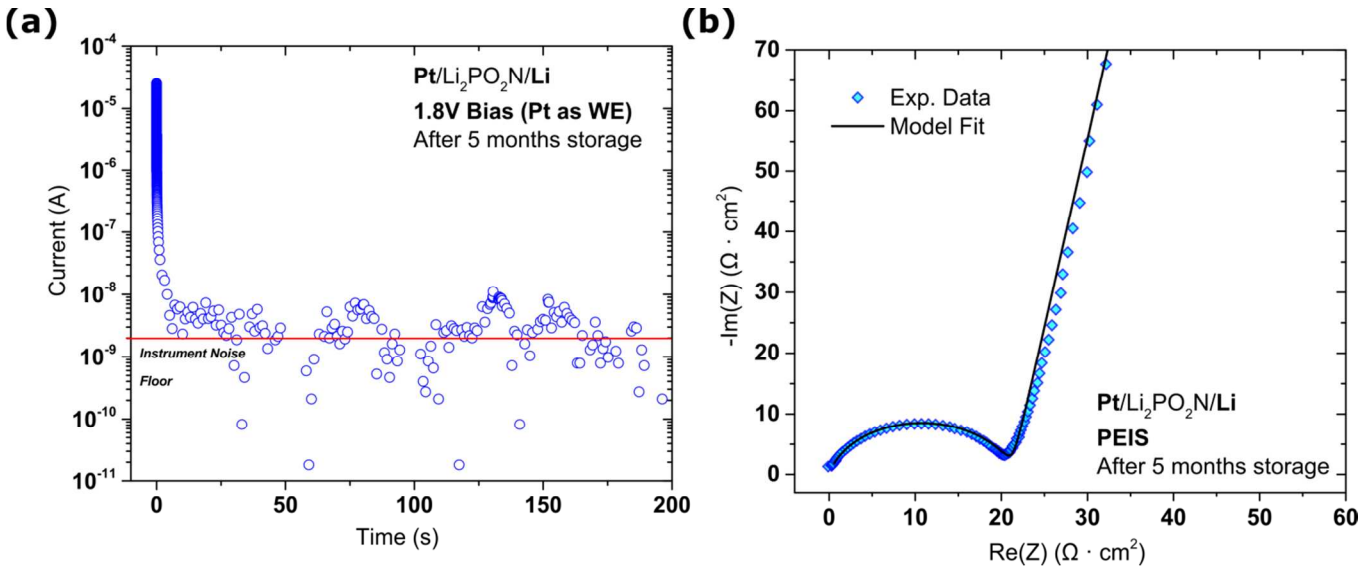

Figure S8: Transport characteristics of a Pt/LPZ-300/Li solid state cell after storage under Ar for 5 months (the same sample characterized in Figure 4b and Figure 5 in the main text). Both chronoamperometry (a) and PEIS (b) indicate that the electrolyte is stable in contact with Li metal for at least months. Measurements were taken at room temperature.

Supplemental References

(1) Kozen, A.; Pearse, A.; Lin, C.-F.; Schroeder, M.; Noked, M.; Lee, S. B.; Rubloff, G. W. Atomic Layer Deposition and In-Situ Characterization of Ultraclean Lithium Oxide and Lithium Hydroxide. *J. Phys. Chem. C* **2014**, *118*.

(2) Talin, A. A.; Ruzmetov, D.; Kolmakov, A.; Mckelvey, K.; Ware, N.; Farid, ‖; Gabaly, E.; Dunn, B.; White, H. S. Fabrication, Testing, and Simulation of All-Solid-State Three- Dimensional Li-Ion Batteries *ACS Applied Materials and Interfaces*.